LU-TP 22-39
June 2022

Spin correlations in top quark pair production at the Large Hadron Collider

Simon Ahlstedt

Department of Astronomy and Theoretical Physics, Lund University

Bachelor thesis supervised by Rikkert Frederix and Leif Gellersen

LUND
UNIVERSITY

Abstract

In this work we investigate the spin correlation effect of the interference between signal and irreducible background events present in top quark pair production at the LHC at LO in the dilepton channel. To simulate the high energy proton-proton collisions of the LHC, MadGraph5_aMC@NLO framework is used as an event generator. The spin correlations are explicitly measured via the lepton kinematics and analyzed through the spin-density formalism. Moreover, we also study the leptonic angular distributions. We find that there is a measurable effect on the spin correlations of top quark pairs from the interference between signal and irreducible background events present in top quark pair production on the order of percent level, but that there is no measurable difference for the leptonic angular distributions.

Popular Science Summary

Atoms often come to mind when thinking of the smallest things in nature. However, atoms are in turn made up of a nucleus of protons and neutrons with orbiting electrons. The protons and neutrons in turn are made up of even smaller fundamental particles called quarks. Together with the leptons, which the electron is a family member of, they make up the fermions, the matter particles. Along with bosons, the particles responsible for the fundamental forces, they make up the Standard Model (SM), which describes most of what we see in our universe, except dark matter and dark energy, which is still unknown.

Arguably, the most peculiar particle in the SM is the top quark. Even though it is unimaginable small, it's about 175 times heavier than the much bigger proton. This immense mass makes it stand out from the rest of the SM. Because of this property, the top quark plays an important role in fine tuning of the SM and can thus be used to probe the underlying physics of the SM. In practice the top quark is hard to produce since by Einsteins famous energy-mass relation, the higher the mass, the more energy is required. Because of this, top quarks can only be produced in high energy collisions. In Earth's upper atmosphere this occurs naturally when cosmic rays collide with particles in the atmosphere. Though, here on earth only the Large Hadron Collider (LHC) at CERN can achieve sufficient energy, just like the Tevatron could in the past.

One property of the top quark is spin, since it can be measured relatively easily via the momentum, angles and directions of the decay products. Spin is an inherent property of all fundamental particles and when a top quark pair is produced their spins are correlated. Even though the pair decays so rapidly that it cannot be measured directly, the spin information is conserved in the decay products. In this way, the top quarks can be measured indirectly by measuring their decay products.

Top quarks are an invaluable tool since they serve as a gateway to understanding current and new physics. Determining the magnitude of the spin effects of the background for top quark pairs is therefore important for the ability to make predictions for observables related to top quarks which in turn can lead to a better understanding of physics. The spin correlation effects of top quark pair production have been measured on numerous levels, however the effect of the interference between signal and background has not yet been considered. The prevailing view is that the effect is negligible and the goal of this work is to confirm or disprove this.

The aim of this project is to quantitatively measure the effect that the interference between signal and background has on the top quark pair's spin correlation. By using the programme MadGraph5_aMC@NLO, proton-proton collisions at the LHC are simulated for the signal and background present in top quark pair production. The spin correlations are then reconstructed from the decay products. In this project we found that there is indeed a measurable effect from the interference between signal and background, however more research is needed in order to determine the origin of these interference effects and if they can be reduced by analysis cuts that select top quark pair production.

Contents

List of acronyms

1. SM Standard Model
2. LHC Large Hadron Collider
3. LO Leading Order

4. NLO Next to Leading Order

5. CM Center of Momentum

6. CP Charge conjugation and Parity

7. NWA Narrow Width Approximation

8. LHE Les Houches Event

List of Figures

List of Tables

1 Introduction

The top quark is the most massive of the particles described by the Standard Model (SM) of particle physics with a mass m_{top}=172.22±0.73 GeV [1]. This gives the top quark some very interesting properties which makes it interesting to investigate for multiple purposes. Firstly, because of its large mass, it has the strongest Higgs-Yukawa-coupling out of all of the SM particles and given the mass-Yukawa coupling relation implies a coupling of $g_t^{SM} \approx 0.99$ when evaluated at the energy scales of m_t [2]. This is interesting since this value lies very near the (quasi-)infrared limit of the SM from which the mass of the top quark can be predicted from. This in turn given a connection between the top quark and the Higgs field which can be used to investigate the Higgs sector [3].

Moreover, the mass of the top quark can be regarded as a free parameter of the SM and this gives it an important role in the fine-tuning problem. Moreover, because of its high mass it has a very small life-time with a mean life-time, τ_t in the range of $1.6 \times 10^{-25} < \tau_t < 6.0 \times 10^{-25}$ that is smaller than the timescale of hadronization, which is 3.3×10^{-24} s [4]. Thus, it decays before hadronization making it an ideal candidate for investigating quark properties. The ability to make predictions for observables related to top quarks is therefore of dire importance both for understanding the existing theories in particle physics and to expand our views of it by extensions to the existing theories. This can in turn lead the way to new physics and theories beyond and within the SM.

Because of its high mass there are few possible reactions for top quarks since the required energy density needed to produce a top quark is immense. The only way to achieve these energy levels is by high energy collisions. Naturally this occurs in the Earth's upper atmosphere when cosmic rays collide with particles in the air creating showers of high energy particles. Top quarks have been detected in numerous high energy collisions since its discovery in 1995 [5] in both single-top and top quark pair production.

Top quark pair production occurs dominantly via strong interaction by gluon-gluon fusion, in which a highly energetic gluon is created which decays into a top (t) and antitop ($\bar{t}$). However, the decay of an intermediate Z boson or photon can also create a top and antitop pair, although this is much rarer. Single top production occurs via weak interaction through several processes, a bottom quark can transform to a top quark by exchanging a W boson with an up or down quark. Furthermore, an intermediate W boson can decay into a top and antibottom quark. Additionally, a single top quark can be produced in association with a W boson which requires an initial state bottom quark.

In top quark pair production when one t and $\bar{t}$ are produced, their spin properties are correlated, making the spin correlation effects an optimal tool to serve as a probe with which one can investigate the underlying physics of the pair. Fortunately, since the mean lifetime of the top quark is smaller than the timescale of hadronization and thus the timescale of interaction, it decays with an almost 100% branching ratio to a W boson and bottom quark before it can interact with particles which would cause spin decorrelation.

This means that spin decorrelation does not set in since the top quark decays before interaction. Because of this, the spin information is conserved in the decay products of the $t\bar{t}$ pair. This makes the decay products an optimal source for understanding the nature of top quarks since it enables an indirect spin correlation measurement of the $t\bar{t}$ pair by measuring the spin correlation of the decay products directly.

The most prominent decay of $t\bar{t}$ pairs is the all-hadronic channel where both W bosons decay into quarks. There is also the less prominent semi-leptonic channel, where one W boson decays into a quark and the other W boson decay to a lepton and neutrino. However, the dilepton channel (with branching ratio $\approx 10.5\%$) where both W bosons decays to a lepton and neutrino results in the clearest signal in hadron-hadron collisions compared to the others decay channels. Thus, the dilepton decay channel is the preferred for investigating spin correlation effects. The top quark spin correlations and the differential distributions of the decay products have previously been studied at various levels of precision through the dilepton channel. The effects of top quark spin correlations have been studied at next to leading order (NLO) at QCD [6, 7, 8], NLOW (NLO QCD + weak) [9] [10] and at NLO (QCD + EW) [11] accuracy. These have also been compared to experimental data at both the ATLAS [12] and CMS [13] experiments.

In these studies, the impact that the interference between signal and background events present in top pair production could have on top pair's spin correlation have not been included in detail. The prevailing view is that the contributions from the interference between signal and background events is essentially insignificant for the spin correlations and therefore it can be omitted. In this study, the spin correlation effect between the double-resonance top quark pair production and the corresponding background events is studied at LO at the Large Hadron Collider (LHC) with 13 TeV center of momentum energy. The aim is to quantitatively determine the effect that the interference between signal and irreducible background events present in top quark pair production have on the spin correlations of top quark pairs. This is done by analysing the dilepton decay channel of top quark pair production. The spin correlations are analyzed numerically through its spin coefficients via the spin-density formalism [10, 14]. To simulate the high energy proton-proton collisions of the LHC, the MadGraph5_aMC@NLO framework [15] is used as an event generator.

The structure of this theses is the following. Firstly in Sec. 2, the theoretical framework of the project is presented, with the model considered in Sec. 2.1, the dilepton decay channel in Sec. 2.2, in Sec. 2.3, the spin correlation coefficients are defined within the spin-density formalism and in Sec. 2.4, the relativistic kinematics of the transformation between the lab frame and the CM frame is explained. Thereafter in Sec. 3 the numerical setup with the different input parameters for MadGraph5_aMC@NLO are explained for the event generation along with the calculated cross sections which are used for weighing the observables. In Sec. 4, the results for the spin coefficients and the distributions of the leptonic angles are presented and discussed. Finally, the results are concluded in Sec. 5.

2 Theoretical setup

In this section, the model considered and the dilepton decay channel of top quark pair production is explained and the processes that are used for analysing the effect between the interference between signal and irreducible background events are presented along with how the different contributions and their cross sections are combined. With the irreducible background we mean all background events that have distributions of the kinematic variables similar to that of the signal that cannot be reduced by applying selection cuts. Furthermore, the analysis for the spin correlation coefficients are introduced, expressed in the spin-density formalism [10, 14]. Thereafter, the relativistic kinematics of the transformation between the lab frame and the $t\bar{t}$ center of momentum (CM) frame is determined.

2.1 Modelling

For this study we have assumed that we have an ideal detector with full reconstruction of the kinematics in the events. Thus, we assume that the t momentum can be reconstructed exactly in each event, despite the fact that we cannot measure the neutrino momentum in experiment. Moreover, since we are interested in the interference effect between the signal and background, we have not restricted the invariant mass of the lepton, b-quark and neutrino to be close to that of the t, something that is always done in practical analysis in order to reduce the contamination from background contributions and the interference between the signal and background. Ergo, we assume that a t can be reconstructed in each event. In addition, the systematical uncertainties are assumed to be exactly the same for all processes. As a result, we are looking at the ideal case, with the best case to find an effect. Hence, there could be that some effects in practice might be washed out a bit compared to the ideal model we consider here.

2.2 The dilepton decay channel

The dilepton decay channel of top quark pair production has contributions from both non-resonant, single-resonant and double-resonant diagrams. With non-resonant contributions we mean the contributions in which we have virtual top quarks that are off-shell as intermediate states in the contributions which do not obey the energy-momentum relation and therefore do not correspond to any resonances in the top field and thus no creation of a t or $\bar{t}$ particle. On the other hand, single-resonant contributions corresponds to the contributions where there is a single-resonance in the top field which corresponds to the creation of a t or $\bar{t}$ particle that is created on-shell as a intermediate state, where the energy-momentum relation is obeyed. Similarly, the double-resonant contribution corresponds to the contributions in which there is a double-resonance in the top field which corresponds to the creation of a $t\bar{t}$ particle pair that is created on-shell as intermediate states, where the energy-momentum relation is obeyed.

The full dilepton decay channel covers all the contributions that produces the dilepton final state $l^+\, l^-\, \nu\, \overline{\nu}\, b\, \overline{b}$ and is denoted by,

$$p\, p \longrightarrow l^+\, l^-\, v_l\, \overline{v_l}\, b\, \overline{b}. \tag{1}$$

In order to study the spin correlation effect of the interference between signal and background present in the top quark pair production, the full dilepton decay process needs to be parameterized for the no interference terms: for the double-resonant contribution, the single-resonant contributions and the non-resonant contributions. The process for the double-resonance contribution which corresponds to the top pair production with its subsequent decays are,

$$p\, p \longrightarrow t\, \overline{t},\ t \longrightarrow l^+\, v_l\, b,\ \overline{t} \longrightarrow l^-\, \overline{v_l}\, \overline{b}. \tag{2}$$

The other contributions can be divided into three distinct processes which can be denoted in a similar manner to the full process described by Eq. (1) with the difference that they all have different exclusions in their s-channels. This is due to the way MadGraph5_aMC@NLO generates processes, since when generating a process one defines what it should include specifically by specifying what to exclude from the process. In this way, when generating the process for the single-resonant t we need to exclude $\bar{t}$ from the s-channel, so that there are no $\bar{t}$ as propagators in the s-channel and thus no $\bar{t}$ as intermediate states in the decay, so only t s-channel resonances are kept. Similarly, for the process that includes the single-resonant $\bar{t}$, t is instead excluded from the s-channel of the process in order to only keep $\bar{t}$ s-channel resonances.

However, in MadGraph5_aMC@NLO, the non-resonant contributions are still included in the processes when we generate the single-resonant t or $\bar{t}$ processes this way, so this in turn gives two contributions which includes both the single + non-resonant contributions for t and $\bar{t}$ respectively. Consequently, the processes cannot be combined directly by simply adding them together since the non-resonant contributions are double counted. Therefore, a third process is needed which excludes both the t and $\bar{t}$ s-channel resonances and only takes into account the non-resonant contributions. This third process can then be subtracted from the other processes in order to correct for the double counting of the non-resonant contributions.

With excluding t and/or $\bar{t}$ in the s-channel, we mean that all the Feynman diagrams which involve t and/or $\bar{t}$ in the s-channel, where two particles join into an t and/or $\bar{t}$ as an intermediate state which then in turn decays into two other particles are discarded, as illustrated in Fig. 1.

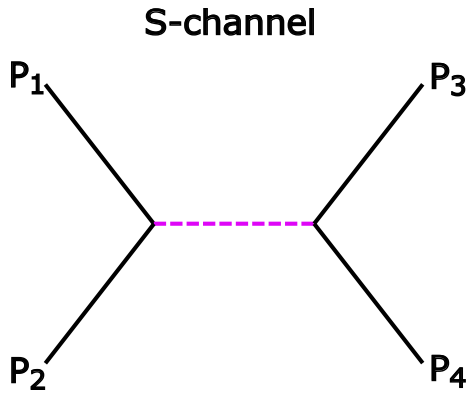

Figure 1: Illustration of the s-channel, where two incoming particles P_1 and P_2 interact, joining into a intermediate particle, here depicted in magenta, which then splits into two new particles P_3 and P_4.

Consequently, this gives a total of five different processes. Namely, one double-resonant (the $t\bar{t}$ pair), two single + non-resonant (one where the t is omitted in the s-channel and one where the $\bar{t}$ is), one non-resonant (both t and $\bar{t}$ excluded in the s-channel), and the full. To get the no interference contribution, the processes are then combined by adding the double-resonant and the two single + non-resonant and then subtracting the non-resonant process in order to account for the double counting of the non-resonant contributions. The cross section for the processes are then related via,

$$\sigma_{\text{Full}} \approx \sigma_D + \sigma_{\setminus t} + \sigma_{\setminus \bar{t}} - \sigma_{\setminus t\bar{t}} \equiv \sigma_{\text{No Interference}}, \tag{3}$$

where σ_{Full}, σ_D, $\sigma_{\setminus t}$, $\sigma_{\setminus \bar{t}}$ and $\sigma_{\setminus t\bar{t}}$ denote the cross sections for the full, Eq. (1), the double-resonant contribution, Eq. (2), the single + non-resonant contribution excluding t in s-channel, the single + non-resonant contribution excluding $\bar{t}$ in the s-channel and the non-resonant contribution excluding both $t\bar{t}$ in the s-channel respectively. These two processes, the full and the no interference which is a combination of the four other contributions are then used in order to analyze the observables related to the irreducible interference between the signal and background events present in top quark production. The cross sections that are to be combined for the no interference are expected to follow a hierarchy in size as,

$$\sigma_D >> \sigma_{\setminus t, \setminus \bar{t}} > \sigma_{\setminus t\bar{t}}. \tag{4}$$

Since the contributions will be weighted towards their cross sections when combined into the no interference, as the cross sections are combined in Eq. (3), the double-resonant process will have the largest contribution toward the observables calculated from the no interference and the non-resonant process will have the smallest contribution to the observables as given by Eq. (4).

In Fig. 2, some example Feynman diagrams of the dilepton decay channel from the different processes are shown, demonstrating the variety of diagrams that are included in the dilepton decay chain with dilepton final states.

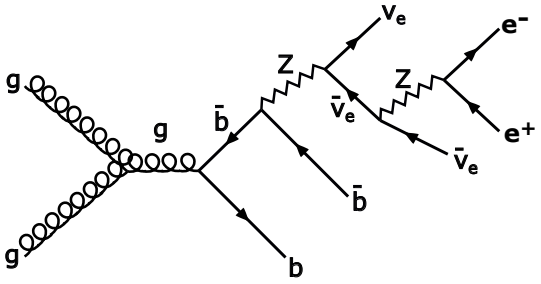

(a) Example Feynman diagram for the full process, Eq. (1).

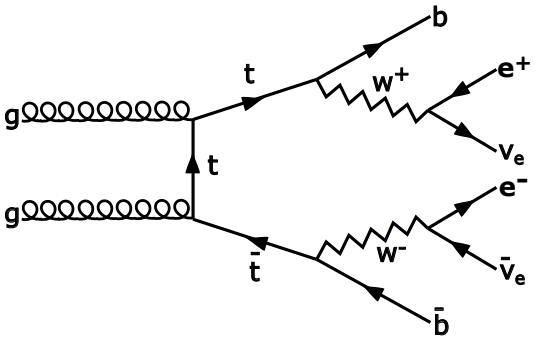

(b) Example Feynman diagram for the double-resonant process, Eq. (2).

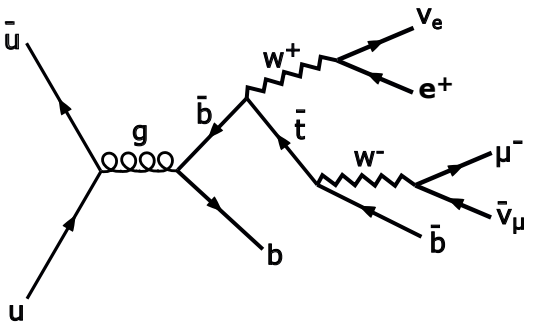

(c) Example Feynman diagram for the single + non-resonant process excluding t in the s-channel.

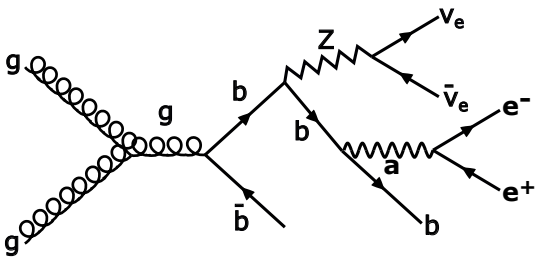

(d) Example Feynman diagram for the single + non-resonant process excluding $\bar{t}$ in the s-channel.

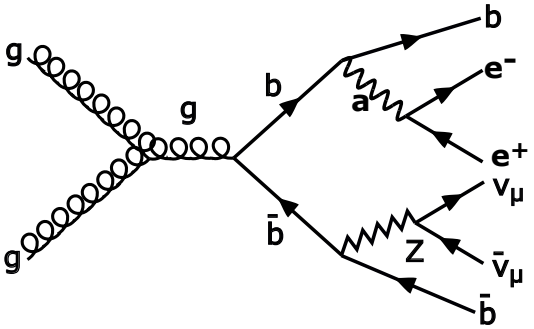

(e) Example Feynman diagram for the non-resonant contribution excluding $t\bar{t}$ in the s-channel.

Figure 2: Examples of Feynman diagrams from the full and the other processes that cover the double-resonant, single-resonant and non-resonant contributions.

2.3 Spin correlation coefficients

The spin correlation effect is analyzed through the use of the spin-density formalism [10, 14], which introduces a set of coefficients which expresses the spin correlations for top quark pair production. The interference effect can then be determined by comparing the spin correlation coefficients between the different contributions. The spin-density formalism introduces a set of coefficients that parametrize the cross section along a chosen axis in a reference frame in which the spins of the top quarks are expressed. In order to present this, a frame of reference that defines the leptonic angles must be introduced. By following the notations used in [10], the orthonormal basis $(\widehat{k}, \widehat{n}, \widehat{r})$ for the spin directions is defined in the following way. Let $\widehat{k}$ be the direction of the top quark in the $t\bar{t}$ CM frame boosted rotation-free from the laboratory frame as the first unit vector. The direction of one of the proton beams in the laboratory frame, denoted $\widehat{p}$ is then used as a helping vector in order to define the second unit vector $\widehat{n}$. The second unit vector is then defined as the normal to the plane spanned by $\widehat{k}$ and $\widehat{p}$ as $\widehat{n}$. Lastly, $\widehat{r}$ is then defined as a unit vector to complete the, right-handed orthonormal basis $(\widehat{k}, \widehat{n}, \widehat{r})$, see Fig. 3.

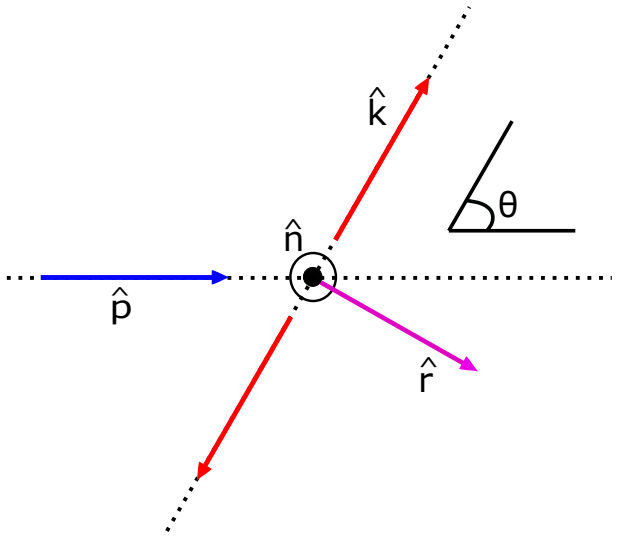

Figure 3: The chosen orthonormal basis for the spin projections, given by $(\widehat{k}, \widehat{n}, \widehat{r})$. The red arrows indicate the directions of the t and $\bar{t}$ in the $t\bar{t}$ CM frame and the first unit vector of the basis, $\widehat{k}$. The black arrow indicates the second unit vector of the basis, $\widehat{n}$ and the magenta arrow shows the third unit vector in the basis, $\widehat{r}$. The blue arrow represents the direction of one of the proton beams in the laboratory frame and the helping vector $\widehat{p}$ which is used to define the orthonormal basis $(\widehat{k}, \widehat{n}, \widehat{r})$. The angle θ is defined as the angle between the outgoing top quark and the direction of the proton beam in the $t\bar{t}$ CM frame.

The unit vectors $\widehat{n}$ and $\widehat{r}$ in the orthonormal basis $(\widehat{k}, \widehat{n}, \widehat{r})$ are thus given by

$$\widehat{n} = \text{sign}(\cos(\theta)) \frac{1}{\sin(\theta)} \widehat{p} \times \widehat{k}. \tag{5}$$

$$\widehat{r} = \text{sign}(\cos(\theta)) \frac{1}{\sin(\theta)} (\widehat{p} - \widehat{k} \cos(\theta)), \tag{6}$$

Where we introduce the sign($\cos(\theta)$) in order to maintain non-vanishing coefficients due to charge conjugation and parity (CP) transformations [10, 14]. Within this frame, the leptonic angles can then be defined as

$$\cos(\theta^k_+) = \widehat{p_{l^+}} \cdot \widehat{k} \qquad \cos(\theta^k_-) = \widehat{p_{l^-}} \cdot \widehat{k} \tag{7}$$

$$\cos(\theta^n_+) = \widehat{p_{l^+}} \cdot \widehat{n} \qquad \cos(\theta^n_-) = \widehat{p_{l^-}} \cdot \widehat{n} \tag{8}$$

$$\cos(\theta^r_+) = \widehat{p_{l^+}} \cdot \widehat{r} \qquad \cos(\theta^r_-) = \widehat{p_{l^-}} \cdot \widehat{r}, \tag{9}$$

where $\widehat{p_{l^\pm}}$ are the direction of motion of the charged leptons and the angles are defined as θ_+ for l^+ and θ_- for l^-. With these definitions, the normalized differential distribution can be expanded in terms of the angles in the following way,

$$\frac{1}{\sigma} \frac{d\sigma}{d\cos(\theta^i_+) d\cos(\theta^j_-)} = \frac{1}{4} \left(1 + B^i_+ \cos(\theta^i_+) + B^j_- \cos(\theta^j_-) + C_{ij} \cos(\theta^i_+) \cos(\theta^j_-)\right), \tag{10}$$

for $i, j = \widehat{k}, \widehat{n}, \widehat{r}$. From this, a set of six B coefficients and nine C coefficients are introduced. By integration and expansion of Eq. (10), one can extract the coefficients via the two following identities,

$$C_{ij} = -9 \frac{\left\langle \cos(\theta^i_+) \cos(\theta^j_-) \right\rangle}{\sigma}, \qquad B^i_\pm = 3 \frac{\left\langle \cos(\theta^i_\pm) \right\rangle}{\sigma}, \tag{11}$$

where -9 and 3 are normalization factors [10] and the $\left\langle \cos(\theta^i_\pm) \right\rangle$ denotes the average of the cosine of the leptonic angles. This is straightforward for the Full contribution, but more complicated for the no interference contributions. In order to get the average leptonic angles and the average products of leptonic angles for the no interference, the separate averages for the individual contributions needs to be weighted with their respective cross section and combined in the same way as the cross sections in Eq. (3). To this end, the averages of the leptonic angles and the averages of the products of the leptonic angles for the no interference are calculated as,

$$\left\langle \cos(\theta^i_\pm) \right\rangle_N = \frac{\sigma_D \left\langle L \right\rangle_D + \sigma_{\setminus t} \left\langle L \right\rangle_{\setminus t} + \sigma_{\setminus \bar{t}} \left\langle L \right\rangle_{\setminus \bar{t}} - \sigma_{\setminus t\bar{t}} \left\langle L \right\rangle_{\setminus t\bar{t}}}{\sigma_N}, \tag{12}$$

and

$$\left\langle \cos(\theta_+^i)\cos(\theta_-^j)\right\rangle_N = \frac{\sigma_D \left\langle L_p\right\rangle_D + \sigma_{\setminus t}\left\langle L_p\right\rangle_{\setminus t} + \sigma_{\setminus \bar{t}}\left\langle L_p\right\rangle_{\setminus \bar{t}} - \sigma_{\setminus t\bar{t}}\left\langle L_p\right\rangle_{\setminus t\bar{t}}}{\sigma_N}, \tag{13}$$

where L and L_p are the cosine of the leptonic angles and the products of the leptonic angles respectively,

$$L = \cos(\theta_\pm^i), \qquad L_p = \cos(\theta_+^i)\cos(\theta_-^j). \tag{14}$$

The spin correlation coefficients for the no interference contributions can then be determined by using Eqs. (12), (13) and (14) in Eq. (11). The code for implementing the spin-density formalism, calculating the coefficients and plotting the distributions of the leptonic angles can be found in appendices A.3, A.4 and A.5 respectively.

2.4 Transformation between the lab frame and the CM frame

The resulting LHE file from the processes containing the events all contain the four-momentum vectors for the initial, the intermediate and the final state particles in the event. In order to determine the spin correlation coefficients as described in Sec. 2.3, the four-momentum vectors needs to be expressed in the $t\bar{t}$ CM frame in order to calculate the leptonic angles described by Eqs. (7), (8) and (9). However, in the LHE file all the four-momentum vectors are measured in the lab frame. Therefore, a Lorentz boost need to be applied to transform the four-momentum vectors from the lab frame, see Fig. 4a, to the $t\bar{t}$ CM frame, see Fig. 4b.

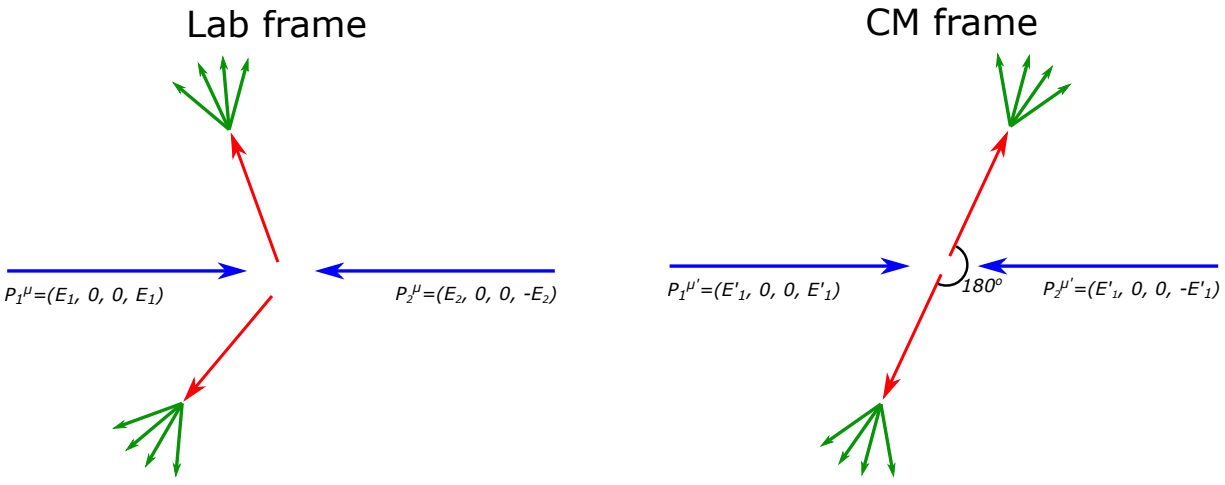

(a) Lab frame. (b) $t\bar{t}$ CM frame.

Figure 4: Comparison between the Lab frame and the $t\bar{t}$ CM frame with the direction of the partons in blue, the direction of the t and $\bar{t}$ in red and the directions of the leptons in green.

In the lab frame, the four-momentum vectors of the two colliding partons have different energies E_1 and E_2 and spacial momentum in opposite directions, equal to its energies, as,

$$P_1^\mu = (E_1, 0, 0, E_1), \qquad P_2^\mu = (E_2, 0, 0, -E_2). \tag{15}$$

Whereas, in the $t\bar{t}$ CM frame, where the top quark pair is back to back, the four-momentum of the partons extracted from the protons must have equal energies and equal spacial momentum in opposite directions, so that the sum of the spatial momenta is zero. So the four-momentum vector of the protons in the $t\bar{t}$ CM frame is then,

$$P_1^{\mu'} = (E_1^{'}, 0, 0, E_1^{'}), \qquad P_2^{\mu'} = (E_1^{'}, 0, 0, -E_1^{'}). \tag{16}$$

The four-momentum vectors of the two frames are related via the Lorentz transformation matrix denoted by $B(u)$ as,

$$P^{\mu'} = B(u)P^\mu, \tag{17}$$

Where u is the velocity of the boost between the two frames as,

$$u = (u_x, u_y, u_z). \tag{18}$$

Since between the Lab frame and the $t\bar{t}$ CM frame, the x and y components remain invariant, the Lorentz transformation only needs to give a boost in the z-direction, with a boost velocity,

$$u = (0, 0, u_z). \tag{19}$$

This in turn gives the Lorentz transformation matrix as

$$B(u) = \begin{bmatrix} \gamma & 0 & 0 & -\beta\gamma \\ 0 & 1 & 0 & 0 \\ 0 & 0 & 1 & 0 \\ -\beta\gamma & 0 & 0 & \gamma \end{bmatrix}, \tag{20}$$

where, β is the boost factor and γ is the Lorentz factor given by,

$$\beta = \frac{u_z}{c}, \qquad \gamma = \frac{1}{\sqrt{1-\beta^2}}. \tag{21}$$

By taking the sum of the four-momentum in each frame for Eqs. (15) and (16) respectively, the transformation between the frames can then be written in matrix form in terms of the Lorentz matrix by using Eqs. (17) and (20) as,

$$\begin{bmatrix} 2E' \\ 0 \\ 0 \\ 0 \end{bmatrix} = \begin{bmatrix} \gamma & 0 & 0 & -\beta\gamma \\ 0 & 1 & 0 & 0 \\ 0 & 0 & 1 & 0 \\ -\beta\gamma & 0 & 0 & \gamma \end{bmatrix} \begin{bmatrix} E_1 + E_2 \\ 0 \\ 0 \\ E_1 - E_2 \end{bmatrix}. \tag{22}$$

Expressing the last row of Eq. (22) and solving for the boost factor gives β in terms of the energies of the partons as,

$$0 = -\beta\gamma(E_1 + E_2) + \gamma(E_1 - E_2) \Rightarrow \beta = \frac{E_1 - E_2}{E_1 + E_2}. \tag{23}$$

The boost matrix between the Lab frame and $t\bar{t}$ CM frame can then be written in terms of the energies of the partons in the Lab frame by using Eqs. (23), (21) and (22) as,

$$B(E_1, E_2) = \begin{bmatrix} \frac{1}{\sqrt{1-(\frac{E_1-E_2}{E_1+E_2})^2}} & 0 & 0 & -\frac{E_1-E_2}{E_1+E_2}\frac{1}{\sqrt{1-(\frac{E_1-E_2}{E_1+E_2})^2}} \\ 0 & 1 & 0 & 0 \\ 0 & 0 & 1 & 0 \\ -\frac{E_1-E_2}{E_1+E_2}\frac{1}{\sqrt{1-(\frac{E_1-E_2}{E_1+E_2})^2}} & 0 & 0 & \frac{1}{\sqrt{1-(\frac{E_1-E_2}{E_1+E_2})^2}}. \end{bmatrix}. \tag{24}$$

With the Lorentz transformation matrix given by Eq. (24) the four-momentum vectors of all the generated particles can be transformed from the lab frame to the $t\bar{t}$ CM frame using Eq. (17). The code for implementing this can be found in appendix A.2.

3 Numerical setup

In this section, the numerical setup of the event generation in MadGraph5_aMC@NLO is described. The syntax for the generation of the different process are explained, together with the different input parameters for the event generation and the relation between the parameters and the processes considered in Sec. 2.2. The cross sections for the processes calculated by MadGraph5_aMC@NLO, which are used for weighting the observables when determining the spin correlation coefficients as described in Sec. 2.3 are also shown. Moreover, the format of the resulting data files from the event generation are remarked upon, along with the formatting of the data for the analysis and determination of the spin correlation coefficients and distributions of the leptonic angles as described in Sec. 2.3.

3.1 Leading Order

MadGraph5_aMC@NLO is used as an event generator to simulate the processes defined in Sec. 2.2. Even though, MadGraph5_aMC@NLO is capable of computing processes at the NLO accuracy, in this study we restrict it to LO only. The reason to this is that simulations at the LO are much simpler and take less time than performing simulations at NLO. Moreover, since we are interested in the interference effects between signal and background in the spin correlations, we do not expect these to be significantly altered by the NLO corrections since the LO terms have the largest contribution and dominates over the NLO terms. Although NLO corrections could show non-zero alterations to the LO, we still want to check for LO effects before going to NLO. Thus, LO accurate simulations are sufficient to investigate if there are a non-trivial interference effects.

3.2 Event generation

The cross section for each event is calculated by the MadGraph5_aMC@NLO program and is performed for a 13 TeV center of momentum energy proton-proton collider. The exact syntax for generating the five processes is as follows,

```
generate p p > l+ l- vl vl~ b b~
generate p p > l+ l- vl vl~ b b~  $$t t~
generate p p > l+ l- vl vl~ b b~  $$t
generate p p > l+ l- vl vl~ b b~  $$t~
generate p p > t t~ , t > l+ vl b , t~ > l- vl~ b~
```

To generate the single resonant+non resonant and the non-resonant processes, the double dollar notation \$\$ is used which excludes t and/or $\bar{t}$ in the s-channel. This means that all diagrams that feature t and/or $\bar{t}$ in the s-channel are discarded and are not taken into account. For the double resonant process, denoted by Eq. (2), the so called decay chain syntax is needed in order to decay the t and $\bar{t}$ into the dilepton final states. Only p-resonant diagrams are included in the computations. P-resonant diagrams are defined by considering the production of p unstable particles u_k $(k = 1, ...p)$ which decay into n_k particles $d_{1,k}, ...d_{n_k,k}$ in association with l stable particles $s_1, ...s_l$ as

$$x + y \longrightarrow u_1(\rightarrow d_{1,1} + ...d_{n_1,1} + X_1) + ...u_p(\rightarrow d_{1,p} + ...d_{n_p,1} + X_p) + s_1 + ..s_l + X_0. \quad (25)$$

Eq. (25) does not properly define a process, but instead corresponds to the contributions to the process,

$$x + y \longrightarrow d_{1,1} + ...d_{n_1,1} + ...d_{1,p} + ...d_{n_p,p} + s_1 + ...s_l + X, \quad (26)$$

$$X = \bigcup_{k=0}^{p} X_k, \tag{27}$$

whose diagrams include an s-channel propagator for each of the p unstable particles u_k, with one end attached to a sub-diagram that contain at least the decay products $d_{1,k}, ...d_{n_k,k}$. These diagrams are so called p-resonant. However, only taking p-resonant diagrams into account for the computations violates gauge invariance. Nonetheless, this can be avoided by using the fact that only using the p-resonant diagrams in computations are formally correct in the limit where all the widths of unstable particles vanish, i.e in the narrow width approximation (NWA), characterized by,

$$\Gamma_{u_k} \longrightarrow 0 \ \ \forall k, \tag{28}$$

where Γ_{u_k} is the decay width for the unstable particle u_k. Furthermore, spin correlations and off-shell effects are both taken into account exactly, but the virtuality m^* of the decayed particle is forced to be in the following range,

$$|m^* - m| \leq \textbf{bwcutoff} \cdot \Gamma, \tag{29}$$

where m is the pole mass, Γ is the resonance/decay width and bwcutoff is a parameter that defines what is considered to be on-shell s-channel resonances and it cuts of the tail of the off-shell effects. The default value of the bwcutoff parameter is 10, however given that the resonance/decay width of the top quark as predicted by the SM when considering $m_t = 172.5$ GeV [4] is given by,

$$\Gamma_t = 1.33 \, \text{GeV}, \tag{30}$$

we set the bwcutoff to 100 in order to maximize the range of the virtuality m^* so that as much as possible effects are taken into account for and to not be that close to the NWA. Furthermore, for the double resonant contribution which have two decay chains for the t and the $\bar{t}$, the hidden parameter cut_decays which by default is set to False, needs to be set to True in order to force MG5aMC to apply the generation cuts also to the t and $\bar{t}$ decay products. Moreover, for a straightforward comparison between the full and no interference contributions we set the renormalization and factorization scales to,

$$\mu_R = \mu_F = m_t = 173 \, \text{GeV}. \tag{31}$$

The number of events for the simulation is chosen as 10^6 events in order to achieve a sufficient statistical significance, which is done by altering the nevents parameter. In summary, all of these changes to the input parameters used in the event generation for the processes are done by running the following commands following the launch of each of the processes,

```
set bwcutoff 100
set fixed_ren_scale true
set fixed_fac_scale true
set scale 173
set dsqrt_q2fact1 173
set dsqrt_q2fact2 173
set cut_decays true
set nevents 1000000
```

The results are Les Houches Event (LHE) files [16] with the unweighted events for the process. In order to compute the spin correlation coefficients as mentioned in Sec. 2.3, we have written a LHE parser in Python, based on the format of the LHE file [17]. It reads the LHE file and converts it to a usable list object containing all the events and the list of all the involved particles and their respective properties that then can be used in the analysis. The code for the LHE parser is listed in appendix A.1.

3.3 Cross sections and re-weighting

The cross sections calculated by MadGraph5_aMC@NLO for the different contributions as given by Eq. (3) which are used for re-weighting the contributions with their respective cross sections when calculating the spin correlation coefficients as in Eq. (11) and for constructing the distributions for the leptonic angles are listed here in Tab. 1.

σ_{Full}	σ_D	$\sigma_{\setminus t}$	$\sigma_{\setminus \bar{t}}$	$\sigma_{\setminus t\bar{t}}$	$\sigma_{\text{No interference}}$
21.6	20.38	0.7426	0.7439	0.0462	21.82

Table 1: The calculated cross sections in pb from the event simulation performed by MadGraph5_aMC@NLO for the different processes and the no interference combination as defined in Eq. (3).

By comparing the cross sections for the full and the no interference as given in Tab. 1, and considering their pure statistical uncertainties, based on the method of integration used by the programme, is on the level of 10^{-4} pb, we can see that there is a difference of about 1% between the cross sections.

4 Results and Discussion

In this section the results for the spin correlation coefficients as defined by Eq. (11) at LO and the distribution of the leptonic angles defined by Eqs. (7), (8) and (9) for the full and the combined no interference processes are presented and compared to each other.

4.1 Correlation coefficients

Here the spin correlation coefficients for the full and the no interference processes are presented together with their corresponding uncertainty defined by the standard error. The B coefficients are shown in Tab. 2 and the C coefficients in Tab. 3.

	Full	**No interference**
B_k^+	$(6.106 \pm 0.007) \times 10^{-2}$	$(6.011 \pm 0.007) \times 10^{-2}$
B_n^+	$(1.9 \pm 0.6) \times 10^{-4}$	$(-3 \pm 57) \times 10^{-6}$
B_r^+	$(-4.11 \pm 0.08) \times 10^{-3}$	$(-3.96 \pm 0.08) \times 10^{-3}$
B_k^-	$(-6.083 \pm 0.007) \times 10^{-2}$	$(-6.015 \pm 0.007) \times 10^{-2}$
B_n^-	$(-9 \pm 6) \times 10^{-5}$	$(-3 \pm 6) \times 10^{-5}$
B_r^-	$(4.27 \pm 0.08) \times 10^{-3}$	$(4.20 \pm 0.08) \times 10^{-3}$

Table 2: The B coefficients as defined by Eq. (11) at LO for the full and the combined no interference processes together with their respective standard error.

	Full	**No interference**
C_{kk}	$(6.003 \pm 0.018) \times 10^{-2}$	$(5.849 \pm 0.017) \times 10^{-2}$
C_{kn}	$(10 \pm 13) \times 10^{-5}$	$(2 \pm 12) \times 10^{-5}$
C_{kr}	$(-3.782 \pm 0.016) \times 10^{-2}$	$(-3.752 \pm 0.015) \times 10^{-2}$
C_{nk}	$(2.7 \pm 1.3) \times 10^{-4}$	$(1.9 \pm 1.2) \times 10^{-4}$
C_{nn}	$(-6.48 \pm 0.08) \times 10^{-3}$	$(-6.67 \pm 0.08) \times 10^{-3}$
C_{nr}	$(1 \pm 10) \times 10^{-5}$	$(-4 \pm 10) \times 10^{-5}$
C_{rk}	$(-3.772 \pm 0.016) \times 10^{-2}$	$(-3.723 \pm 0.015) \times 10^{-2}$
C_{rn}	$(-3 \pm 10) \times 10^{-5}$	$(-2 \pm 1) \times 10^{-4}$
C_{rr}	$(-7.561 \pm 0.014) \times 10^{-2}$	$(-7.491 \pm 0.013) \times 10^{-2}$

Table 3: The C coefficients as defined by Eq. (11) at LO for the full and the combined no interference processes together with their respective standard error.

Firstly, by looking at Tab. 2 it is clear that most of the B coefficients for both the full and the no interference processes are quite small, with some being compatible with zero at LO, and most of them are on a order lower than 10^{-3}. Despite this, four of the coefficients, namely the B_k^+, B_k^-, B_r^+ and B_r^- coefficients for the full and the no interference processes are non-compatible with zero, with the smallest out of them being on an order of 10^{-3}. A similar trend can be seen in Tab. 3 for the C coefficients, where most of the coefficient for both the full and the no interference processes are compatible with zero at LO, being on the order of 10^{-3} or lower. However, the C_{kk}, C_{kr}, C_{rk} and C_{rr} coefficients for both the full and the no interference processes are all on the order of magnitude of 10^{-2}. The standard error for all of the B and C coefficients for both the full and no interference processes are all on the order of 10^{-4} to 10^{-5} and as a result, the coefficients of order 10^{-3} or greater have an smaller error estimate compared to the smaller coefficients that are compatible with zero which are as small as 10^{-6}, making their associated standard error of the same size or even greater than the the calculated value of the coefficients.

Beginning with the B coefficients in Tab. 2, it is evident that when taking into account the uncertainties in the coefficients almost all of the coefficients, specifically 4 out of 6 are compatible with each other when comparing the values for the full and the no interference contributions. Nonetheless, one can see that there is in fact a difference for the largest B coefficients, namely the B_k^+ and B_k^-. When comparing the coefficients for the two contributions and taking into account their respective uncertainties one can see that there is a difference on the order of percent level for the coefficients. Furthermore, by looking at Tab. 3, one can again see that most of the coefficients when comparing the two contributions are compatible with each other when taking into account the uncertainties. Even so, one can see that there is an difference in the four of the larger coefficients, namely in C_{kk}, C_{nn}, C_{rk} and C_{rr} when comparing the two contributions to each other. When taking into account the uncertainties one can see that there is a difference between the coefficients on the order of percent level for C_{kk}, C_{nn}, C_{rk} and C_{rr} when comparing the full and the no interference contributions. Thus, from Tab. 2 and Tab. 3 it is evident that there is an difference in the spin correlations between the full and the no interference contributions on the order of percent level.

4.2 Distributions of the leptonic angles

Here the results for the distributions for the leptonic angles defined by Eqs. (7), (8) and (9) are plotted as histograms for the full and the combined no interference processes normalized and weighted with their respective cross sections as defined in Eq. (3) and calculated in Tab. 1. The ratio between the bin counts of the no interference and the full is also plotted for each histogram in order to visualize the compatibility between the no interference and the full processes.

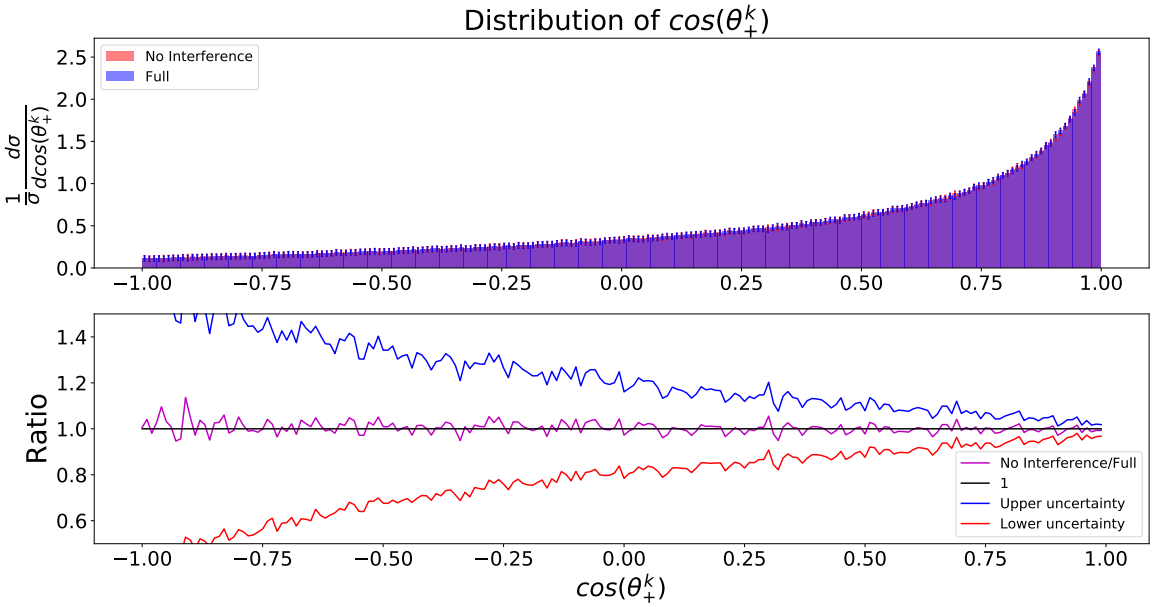

(a) In the upper subplot is the normalized distribution of $\cos(\theta^k_+)$ for the full process in blue and the no interference process in red, weighted with their respective cross sections. The error bars show the standard error and are depicted in blue for the full and in red for the no interference process. The lower subplot depicts in magenta, the ratio between the bin counts of the no interference and the full processes. The uncertainties for the ratio is shown in blue and red for the upper and lower uncertainty respectively.

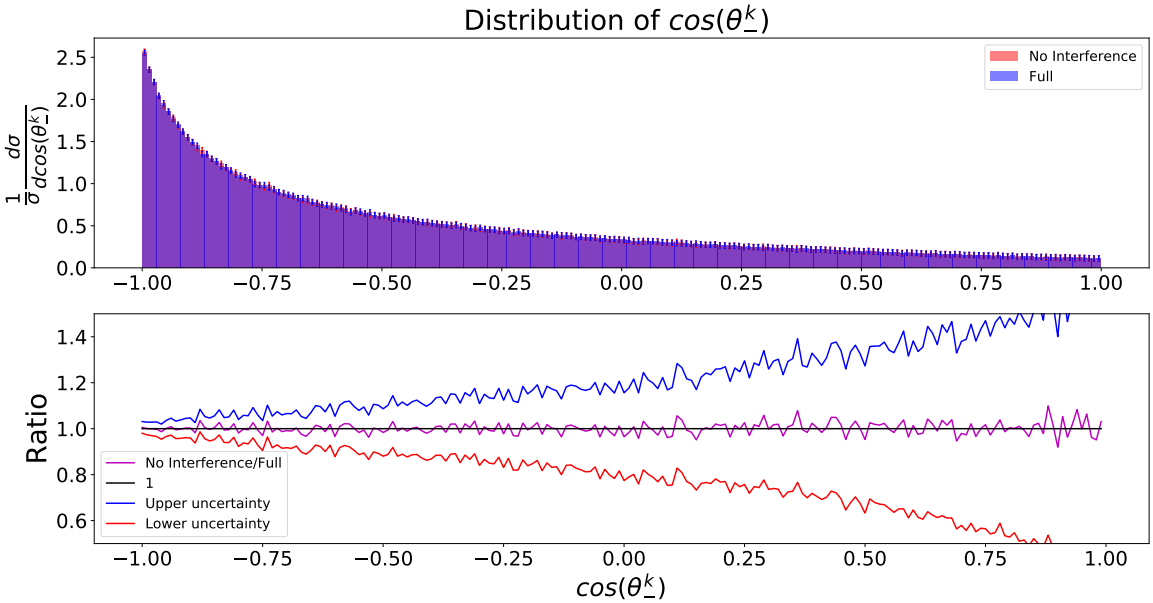

(b) In the upper subplot is the normalized distribution of $\cos(\theta^k_-)$ for the full process in blue and the no interference process in red, weighted with their respective cross sections. The error bars show the standard error and are depicted in blue for the full and in red for the no interference process. The lower subplot depicts in magenta, the ratio between the bin counts of the no interference and the full processes. The uncertainties for the ratio is shown in blue and red for the upper and lower uncertainty respectively.

Figure 5: The normalized and weighted distributions for the positive and negative leptonic angles in the $\widehat{k}$ direction as defined by Eq. (7), together with the ratio plot between the no interference and the full.

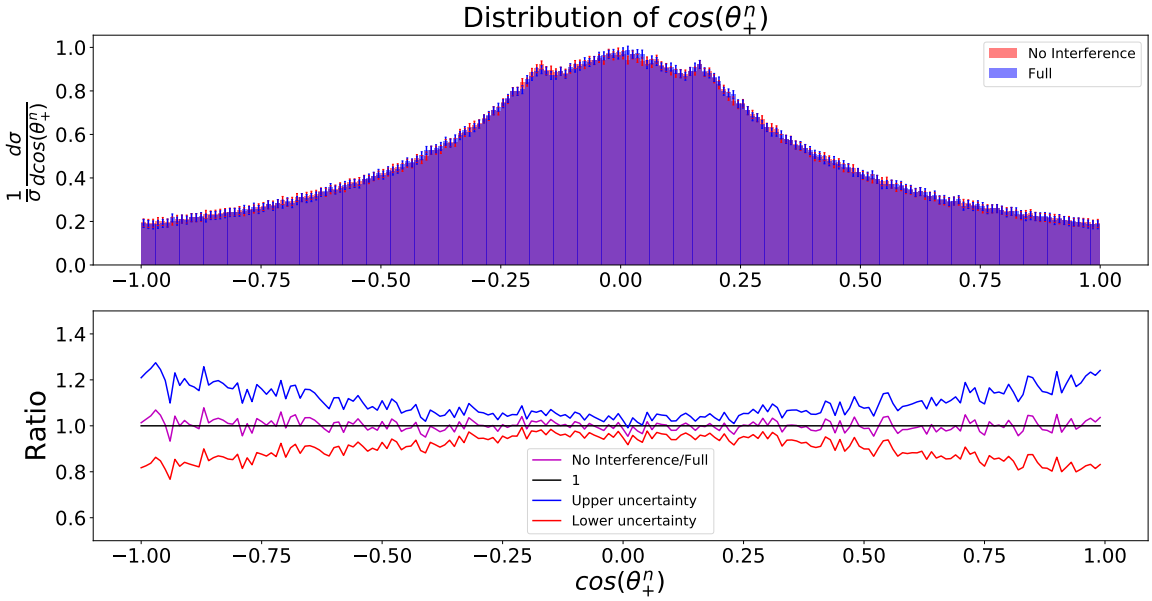

(a) In the upper subplot is the normalized distribution of $\cos(\theta^n_+)$ for the full process in blue and the no interference process in red, weighted with their respective cross sections. The error bars show the standard error and are depicted in blue for the full and in red for the no interference process. The lower subplot depicts in magenta, the ratio between the bin counts of the no interference and the full processes. The uncertainties for the ratio is shown in blue and red for the upper and lower uncertainty respectively.

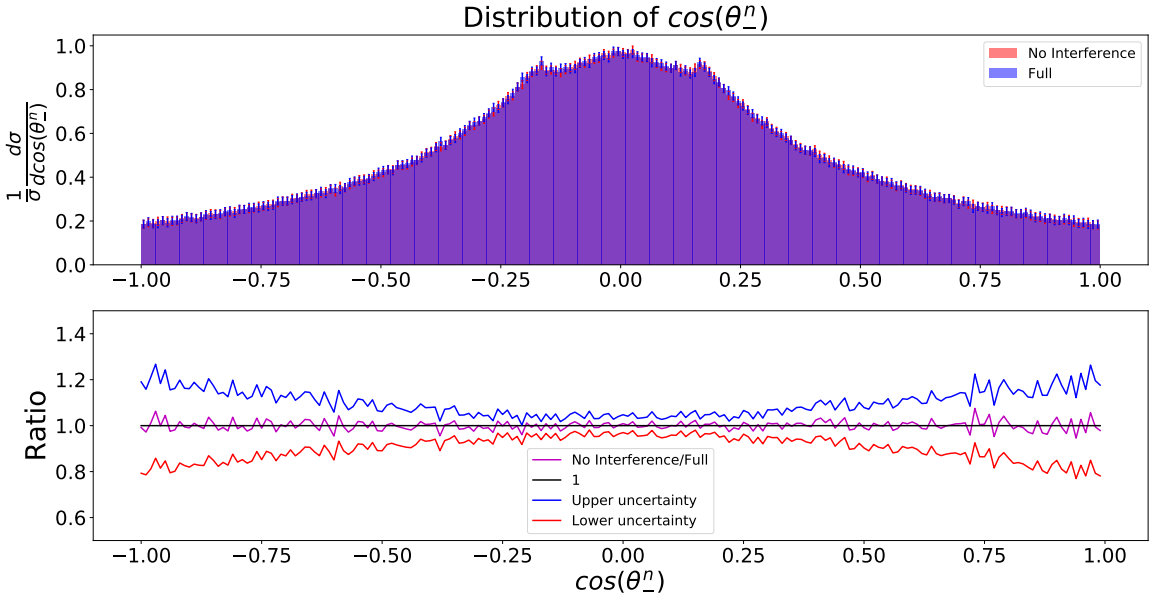

(b) In the upper subplot is the normalized distribution of $\cos(\theta^n_-)$ for the full process in blue and the no interference process in red, weighted with their respective cross sections. The error bars show the standard error and are depicted in blue for the full and in red for the no interference process. The lower subplot depicts in magenta, the ratio between the bin counts of the no interference and the full processes. The uncertainties for the ratio is shown in blue and red for the upper and lower uncertainty respectively.

Figure 6: The normalized and weighted distributions for the positive and negative leptonic angles in the $\widehat{n}$ direction as defined by Eq. (8), together with the ratio plot between the no interference and the full.

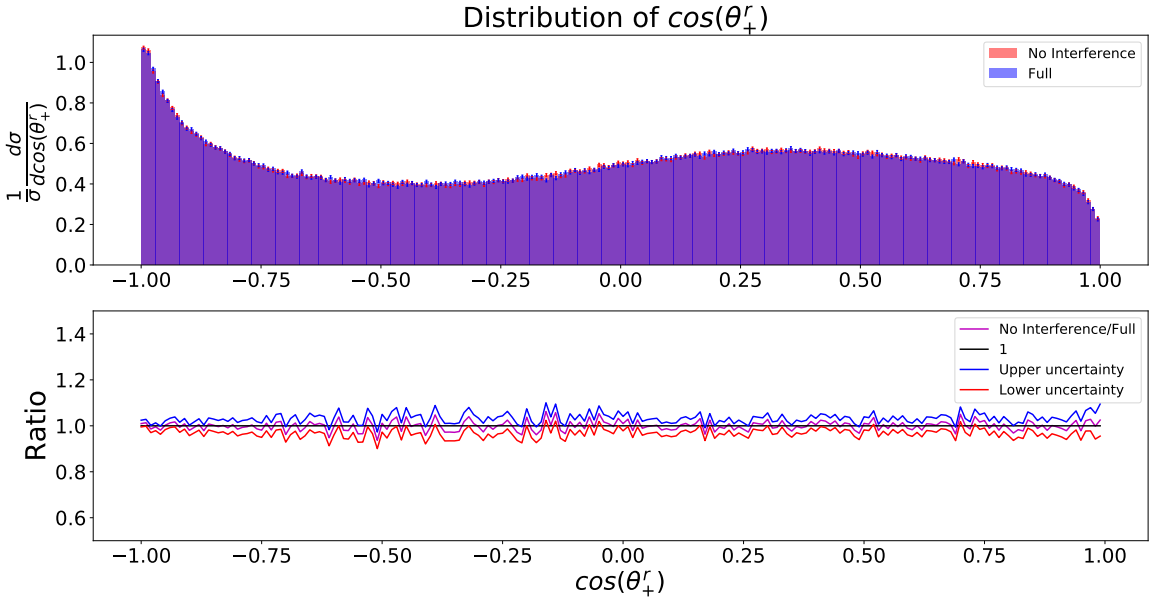

(a) In the upper subplot is the normalized distribution of $\cos(\theta^r_+)$ for the full process in blue and the no interference process in red, weighted with their respective cross sections. The error bars show the standard error and are depicted in blue for the full and in red for the no interference process. The lower subplot depicts in magenta, the ratio between the bin counts of the no interference and the full processes. The uncertainties for the ratio is shown in blue and red for the upper and lower uncertainty respectively.

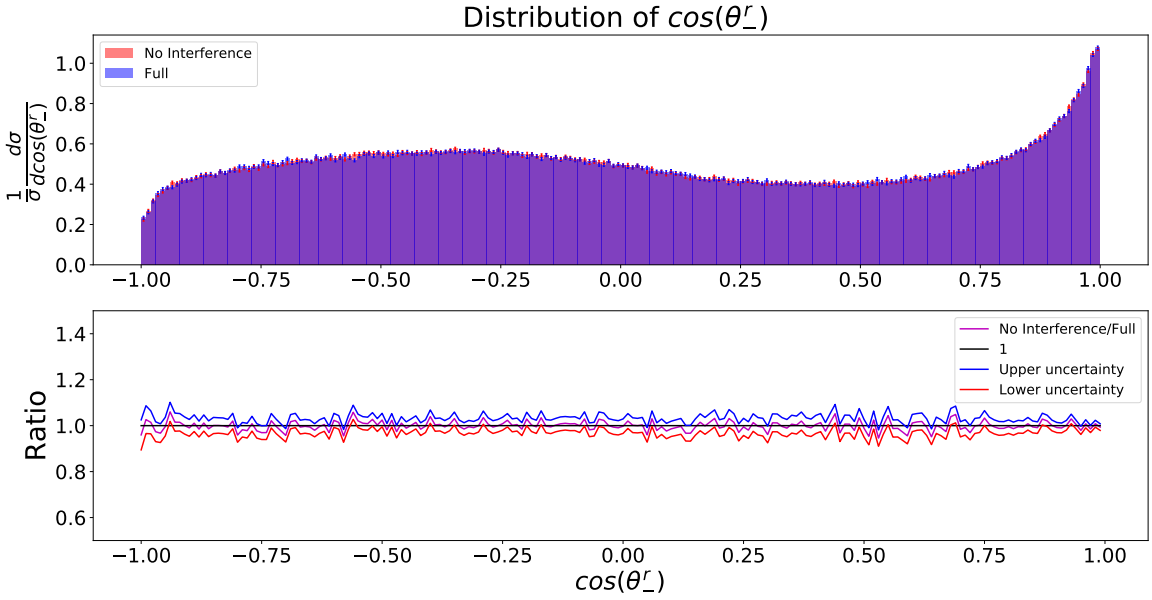

(b) In the upper subplot is the normalized distribution of $\cos(\theta^r_-)$ for the full process in blue and the no interference process in red, weighted with their respective cross sections. The error bars show the standard error and are depicted in blue for the full and in red for the no interference process. The lower subplot depicts in magenta, the ratio between the bin counts of the no interference and the full processes. The uncertainties for the ratio is shown in blue and red for the upper and lower uncertainty respectively.

Figure 7: The normalized and weighted distributions for the positive and negative leptonic angles in the $\widehat{r}$ direction as defined by Eq. (9), together with the ratio plot between the no interference and the full.

Firstly, by looking at Fig. 5 one can see that the the two histograms are mirror symmetric with respect to each other which is to be expected given the definition of $\widehat{k}$. In a similar manner one can also see in Fig. 7 that the shape of the histograms also are mirror symmetric with respect to each other which is to be expected given how the $\widehat{r}$ vector was defined as in Eq. (5). Moreover, as is seen in Fig. 6, the leptonic distributions for $\cos(\theta^n_+)$ and $\cos(\theta^n_-)$ are the only ones that are symmetric with respect to each other compared to the two other sets of distributions for the positive and negative leptonic angles. This is however to be expected given how the $\widehat{n}$ vector was constructed as seen in Eq. (6).

Looking at the leptonic distributions in the $\widehat{k}$ direction in Fig. 5, one can see that when taking into account the uncertainties, both the distributions for $\cos(\theta^k_+)$ and $\cos(\theta^k_-)$ are compatible with each other when comparing the full and the no interference contributions. Additionally, looking at the ratio plots between the no interference and the full in Fig. 5, for both $\cos(\theta^k_+)$ and $\cos(\theta^k_-)$ shows a ratio very close to 1, with only small deviations from 1. However, when considering the uncertainties for the ratio between the no interference and the full, the ratio falls within a ratio of 1. This in turn points to the fact that the distributions are compatible with each other. Furthermore, this behaviour can also be seen in the leptonic distribution for $\cos(\theta^n_+)$ and $\cos(\theta^n_-)$ in Fig. 6, where it is evident that the distribution are compatible for the full and the no interference contributions when taking into account the uncertainties. The ratio plots between both $\cos(\theta^n_+)$ and $\cos(\theta^n_-)$ as seen in Fig. 6 are also very close to 1, with only small deviations from 1, which in turn is accounted for when considering the uncertainties for the ratio. This also comes to show that the distributions are compatible. Moreover, for the leptonic distribution of $\cos(\theta^r_+)$ and $\cos(\theta^r_-)$ in Fig. 7, it is also clear that the distributions for the full and the no interference are compatible with each other when considering the uncertainties. Similarly, looking at the ratio plots of $\cos(\theta^r_+)$ and $\cos(\theta^r_-)$ in Fig. 7 one can see that the ratio plots are close to 1 with only small deviations from 1 which is accounted for when including the uncertainties. Hence, from Fig. 5, Fig. 6 and Fig. 7 it is evident that there is no measurable difference between the leptonic distributions of the full and the no interference contributions.

Given that the spin correlation coefficients are highly correlated with the leptonic distributions, since the coefficients are a combination of the distributions, making them directly dependent on each other, makes it a bit surprising that we measure a detectable effect between the spin correlation coefficients but not for the leptonic distributions. On the other hand, this is most likely due to the fact that the statistical fluctuations in the differential distributions are simply too large to see an effect for, similar to what could be seen in [11].

5 Conclusion

Here for the first time we investigate the effect that the interference between signal and irreducible background events present in top quark pair production have on the spin correlations of top quark pairs. We have focused on the top quark pair production and decay to a dilepton channel at LO. There are two major approximations that we have used, primarily that we have assumed an ideal detector and secondly, that we can reconstruct the top quark momentum exactly, even though we cannot measure the neutrino momentum in experiment. Furthermore, we have not restricted the invariant mass between the lepton, b-quark and neutrino to be close to that of the top quark, something that in practical analysis always will be done in order to reduce the contamination from background contributions even more. This would also reduce the contribution from the interference between the signal and background. Hence, we are only looking at the ideal case, i.e., the best case to find an effect. For this reason, in practice some effects might be washed out a bit compared to the ideal model considered here. Additionally, one can note that the $$ is more limited than other alternatives such as $ for the event generation, although it cannot be considered an approximation per se, since it is necessary in order to define and generate the no interference contributions. Even with all of this, the calculated cross sections for the full and the combined no interference contributions are compatible within 1 %, indicating that the $$ and its associated parameter changes works in this context.

To this end, we investigated the effect on the spin correlations of top quark pairs within the spin-density formalism that the interference between signal and irreducible background events present in top quark pair production have. We found that for the spin correlation coefficients most of the coefficients are compatible with zero for both the full and the no interference contributions. However, a number of coefficients that deviates from zero do have a significant difference on the order of percent level between the full and the no interference contributions, which indicates that there is an effect from the interference between signal and background events present in top quark pair production on the spin correlations of top quark pairs. Additionally, the distributions of the positive and negative leptonic angles in all $\widehat{k}$, $\widehat{n}$ and $\widehat{r}$ directions are all compatible with each other for the full and the no interference.

All in all considering this ideal model, the results, with the differences for the spin correlation coefficients between the full and the no interference contributions indicates that the interference between signal and irreducible background events present in top quark pair production do in fact have an measurable effect on the order of percent level on the spin correlation of top quark pairs. This challenges the notion up till now, that the effect from the interference between signal and background on the spin correlation of top quark pairs can be neglected in relation to the top quark pairs spin correlations. In conclusion, more investigations are needed in order to determine the origins of these interference effects and if they can be reduced by analysis cuts that select top quark pair production or not.

A Appendices

A.1 LHE parser Python

```
import re
from typing import NamedTuple
import numpy as np

EVENT_TAG = '<event>'
INIT_TAG = '<init>'
INIT_END_TAG = '</init>'
FILE_END_TAG = '</LesHouchesEvents>'

class Parameters(NamedTuple):
    id_a : int # IDBMUP(1)
    id_b : int # IDBMUP(2)
    energy_a : float # EBMUP(1)
    energy_b : float # EBMUP(2)
    pdfgup_a : int # PDFGUP(1)
    pdfgup_b : int # PDFGUP(2)
    pdfsup_a : int # PDFSUP(1)
    pdfsup_b : int # PDFSUP(2)
    weight : int # IDWTUP
    nprup : int # NPRUP
    xsecup : float # XSECUP(MAXPUP)
    xerrup : float # XERRUP(MAXPUP)
    xmaxup : float # XMAXUP(MAXPUP)
    lprup : float # LPRUP(MAXPUP)

class Particle(NamedTuple):
    pdgid : int # IDUP
    status : int # ISTUP
    mother_a : int # MOTHUP(1)
    mother_b : int # MOTHUP(2)
    color_a : int # ICOLUP(1)
    color_b : int # ICOLUP(2)
    px : float # PUP(1)
    py : float # PUP(2)
    pz : float # PUP(3)
    E : float # PUP(4)
    M : float # PUP(5)
    lifetime : float # VTIMUP
    spin : float # SPINUP

class Event(NamedTuple):
    nparticles : int # NUP
    subprocess : int # IDPRUP
    weight : float # XWGTUP
    scale : float # SCALUP
    qedcoupling : float # AQEDUP
    qcdcoupling : float # AQCDUP
    particles : list # List of particles in the event

class Process(NamedTuple):
    init : Parameters
    events : list


# Reads LHEF file and stores the information in according classes
def ReadLHEF(filepath):
    fp = open(filepath)
    init = []
    line = fp.readline()

    while line.strip() != INIT_TAG: line = fp.readline()
    line = fp.readline()
```

```
    while line.strip() != INIT_END_TAG: # Reads the initialisation parameters
        if "<generator" in line:
            line=fp.readline()
            continue
        line = re.sub('\s+', ' ', line).strip().split(' ')
        line = [float(i) for i in line]
        init = init + line
        line = fp.readline()


    p = Process(Parameters(*init),[])

    line = fp.readline()
    while line.strip() != FILE_END_TAG: # Reads the events
        if line.strip() == EVENT_TAG:
            line = fp.readline()
            line = re.sub('\s+', ' ', line).strip().split(' ')
            line[0:2] = map(int, line[0:2])
            line[2:6] = map(float, line[2:6])
            e = Event(*line, [])

            for i in range(e.nparticles):
                line = fp.readline()
                line = re.sub('\s+', ' ', line).strip().split(' ')
                line[0:6] = map(int, line[0:6])
                line[6:13] = map(float, line[6:13])

                e.particles.append(Particle(*line))

            p.events.append(e)

        line = fp.readline()

    return p

#The parser can then be used to read the LHE files by using;
Data=ReadLHEF("LHE_File_path")
```

A.2 Lab frame to CM frame transformation

```
#Gives the list of each particles for event i in Data.
def Compact_events(self, i):
    return self.events[i][6]

#Gives the list of initial particles for event i in Data
def Initial_particles(self,i):
    list=Compact_events(self,i)
    array=[]
    for j in range(len(list)):
        if list[j][1]==-1:
            array.append([list[j].pdgid, list[j].status,  [list[j].E,
            list[j].px, list[j].py, list[j].pz]])
    return array

#Gives the list of intermediate particles for event i in Data
def Intermediate_particles(self,i):
    list=Compact_events(self,i)
    array=[]
    for j in range(len(list)):
        if list[j][1]==2:
            array.append([list[j].pdgid, list[j].status, [list[j].E,
            list[j].px, list[j].py, list[j].pz]])
    return array

#Gives the list of final particles for event i in Data
```

```
def Final_particles(self,i):
    list=Compact_events(self,i)
    array=[]
    for j in range(len(list)):
        if list[j][1]==1:
            array.append([list[j].pdgid, list[j].status, [list[j].E,
            list[j].px, list[j].py, list[j].pz]])
    return array
#The Lorentz boost between Lab frame and CM frame
# The beta value for the boost for event i
def Beta(self,i):
    list=Initial_particles(self,i)
    E_1=list[0][2][0]
    E_2=list[1][2][0]
    Beta=(E_1-E_2)/(E_1+E_2)
    return Beta

#The gamma factor for the boost for event i
def Gamma_factor(self,i):
    Gamma=1/np.sqrt(1-Beta(self,i)**2)
    return Gamma

# The boost in z-direction from the lab frame to the Cm frame
def Boost_matrix(self,i):
    g=Gamma_factor(self,i)
    b=Beta(self,i)
    Boost_matrix=[ [g,     0,    0,      -b*g],
                   [0,     1,    0,      0   ],
                   [0,     0,    1,      0   ],
                   [-b*g,  0,    0,      g   ]
                 ]
    return Boost_matrix

#Boost the initial state particles from the Lab frame to the CM frame.
def Boost_ini(self,i):
    t=Boost_matrix(self,i)
    list=Initial_particles(self, i)
    b=[]
    for j in range(len(list)):
        l=list[j][2]
        boosted=np.dot(t,l)
        new=[list[j][0], list[j][1], boosted]
        b.append(new)
    return b

#Boost the intermediate state particles from the Lab frame to the CM frame.
def Boost_int(self,i):
    t=Boost_matrix(self,i)
    list=Intermediate_particles(self,i)
    b=[]
    for j in range(len(list)):
        l=list[j][2]
        boosted=np.dot(t,l)
        new=[list[j][0], list[j][1], boosted]
        b.append(new)
    return b

#Boost the final state particles from the Lab frame to the CM frame.
def Boost_final(self,i):
    t=Boost_matrix(self,i)
    list=Final_particles(self,i)
    b=[]
    for j in range(len(list)):
        l=list[j][2]
        boosted=np.dot(t,l)
        new=[list[j][0], list[j][1], boosted]
        b.append(new)
    return b
```

```
#Reconstructing the top for each event
def Top_reconstruction(self,i):
    l=Boost_final(self,i)
    list=[]
    for j in range(len(l)):
        if l[j][0]==5 or l[j][0]==-11 or l[j][0]==-13 or l[j][0]==12 or l[j][0]==14:
            list.append(l[j])
    top=0
    for k in range(len(list)):
        top=top+list[k][2]
    return top
```

A.3 The spin-density formalism

```
#Constructing the unit vectors for the spin density formalism
# The normalised vector of the incoming proton from the left, i.e the beam axis
def p_hat(self,i):
     p=Boost_ini(self,i)[0][2] # Incoming proton from the left
     proton=[p[1], p[2], p[3]]
     p_hat=proton/np.linalg.norm(proton)
     return p_hat

#The k_hat basis vector for the orthornormal basis (k,n,r)
def k_hat(self,i):
    t=Top_reconstruction(self,i)
    top=[t[1], t[2], t[3]]
    k_hat=top/np.linalg.norm(top)
    return k_hat

#The angle between the beam axis and the outgoing top quark
def Theta(self,i):
    p=p_hat(self,i)
    k=k_hat(self,i)
    Cos_theta=np.dot(p, k)
    return Cos_theta

#The n_hat basis vector for the orthornormal basis (k,n,r)
def n_hat(self,i):
    cos_theta=Theta(self,i)
    theta=np.arccos(cos_theta)
    p=p_hat(self,i)
    k=k_hat(self,i)
    n_hat=np.sign(cos_theta)*(1/np.sin(theta))*np.cross(p,k)
    return n_hat

#The r_hat basis vector for the orthornormal basis (k,n,r)

def r_hat(self,i):
    cos_theta=Theta(self,i)
    theta=np.arccos(cos_theta)
    p=p_hat(self,i)
    k=k_hat(self,i)
    r_hat=np.sign(cos_theta)*(1/np.sin(theta))*(p-k*cos_theta)
    return r_hat

# Defining the Leptonic angles
#The first list is the positive leptonic angles (k,n,r) and
#the second are the negative leptonic angles (k,n,r)
def Leptonic_angles(self,i):
    k=k_hat(self,i)
    n=n_hat(self,i)
    r=r_hat(self,i)
    f=Final_particles(self,i)
```

```
    for j in range(len(f)):
        if f[j][0]==-11 or f[j][0]==-13:
            pos=f[j]
        if f[j][0]==11 or f[j][0]==13:
            neg=f[j]

    Pos=[pos[2][1], pos[2][2], pos[2][3]] #Pos leptonic momentum vector
    Neg=[neg[2][1], neg[2][2], neg[2][3]] #Neg leptonic momentum vector
    Pos_hat=Pos/np.linalg.norm(Pos) # The normalized pos leptonic momentum #vector
    Neg_hat=Neg/np.linalg.norm(Neg)  # The normalized neg leptonic momentum #vector

    #The pos leptonic angles
    cos_pos_k=np.dot(Pos_hat, k)
    cos_pos_n=np.dot(Pos_hat, n)
    cos_pos_r=np.dot(Pos_hat, r)

    #the neg leptonic angles
    cos_neg_k=np.dot(Neg_hat, k)
    cos_neg_n=np.dot(Neg_hat, n)
    cos_neg_r=np.dot(Neg_hat, r)
    return [[cos_pos_k, cos_pos_n, cos_pos_r], [cos_neg_k, cos_neg_n,  cos_neg_r]]

def Bin_angles(self):
    Angles=[]
    A=[ [ [], [], [] ] , [ [], [], [] ] ]
    for i in range(len(self.events)):
        L=Leptonic_angles(self, i)
        Angles.append(L)
    for i in range(len(Angles)):
        for j in range(len(Angles[i])):
            for k in range(len(Angles[i][j])):
                A[j][k].append(Angles[i][j][k])
    return A

#In order to cut doum on compilation time and the heavy use of memory, the
#leptonic angles were calculated separately for each of the event files
#and saved to a new txt file which then later could be accessed.


#Saving the leptonic angles into empty txt files.
with open('Full_bin_angles.txt', 'w') as f:
     f.write(json.dumps(Bin_angles(Full)))

with open('No_t_bin_angles.txt', 'w') as f:
     f.write(json.dumps(Bin_angles(No_t)))

with open('No_t_bar_bin_angles.txt', 'w') as h:
     h.write(json.dumps(Bin_angles(No_t_bar)))

with open('No_tt_bin_angles.txt', 'w') as m:
     m.write(json.dumps(Bin_angles(No_t_t_bar)))


with open('Signal_bin_angles.txt', 'w') as n:
     n.write(json.dumps(Bin_angles(Signal)))


#Loading the leptonic angles for the event files
with open('Full_bin_angles.txt', 'r') as f:
    theta_Full = json.loads(f.read())

with open('No_t_bin_angles.txt', 'r') as g :
    theta_No_t=json.loads(g.read())


with open('No_t_bar_bin_angles.txt', 'r') as h:
    theta_No_tb= json.loads(h.read())
```

```
with open('No_tt_bin_angles.txt', 'r') as m:
    theta_No_tt= json.loads(m.read())

with open('Signal_bin_angles.txt', 'r') as n:
    theta_Sig= json.loads(n.read())

#theta on the form:
#[[theta_k_p_list, theta_n_p_list, theta_r_p_list] ,
#[[theta_k_n_list, theta_n_n_list, theta_r_n_list]]]
```

A.4 The spin correlation coefficients

```
Sigma_Full=21.5987986019
Sigma=[0.742564387287,  0.743885881147, 0.0461979366247, 20.3763 ]
Sigma_No_int=Sigma[0]+Sigma[1]-Sigma[2]+Sigma[3]

av_theta_Full=[ [ [], [], [] ], [ [], [], [] ]]
av_theta_No_t=[ [ [], [], [] ], [ [], [], [] ]]
av_theta_No_tb=[ [ [], [], [] ], [ [], [], [] ]]
av_theta_No_tt=[ [ [], [], [] ], [ [], [], [] ]]
av_theta_Sig=[ [ [], [], [] ], [ [], [], [] ]]

for i in range(len(theta_Full)):
    for j in range(len(theta_Full[i])):
        av_theta_Full[i][j].append(np.average(theta_Full[i][j]))
        av_theta_No_t[i][j].append(np.average(theta_No_t[i][j]))
        av_theta_No_tb[i][j].append(np.average(theta_No_tb[i][j]))
        av_theta_No_tt[i][j].append(np.average(theta_No_tt[i][j]))
        av_theta_Sig[i][j].append(np.average(theta_Sig[i][j]))

av_theta_No_t_w=np.multiply(av_theta_No_t, Sigma[0])
av_theta_No_tb_w=np.multiply(av_theta_No_tb, Sigma[1])
av_theta_No_tt_w=np.multiply(av_theta_No_tt, Sigma[2])
av_theta_Sig_w=np.multiply(av_theta_Sig, Sigma[3])

#Taking the sum of the averages to get the average of the sum for
#the no interference as a combination of the sub processes

av_theta_No_int=[[0,0,0], [0,0,0]]

for i in range(len(av_theta_No_t_w)):
    for j in range(len(av_theta_No_t_w[i])):
        av_theta_No_int[i][j]=(av_theta_No_int[i][j]+av_theta_No_t_w[i][j]
        +av_theta_No_tb_w[i][j]-av_theta_No_tt_w[i][j]+
        av_theta_Sig_w[i][j])/Sigma_No_int

n_B_No_int=3/Sigma_No_int
n_B_Full=3/Sigma_Full
B_No_int=np.multiply(n_B_No_int, av_theta_No_int)
B_Full=np.multiply(n_B_Full, av_theta_Full)

#The C coefficients
theta_p_Full=[ [ [], [], [] ], [ [], [], [] ], [ [], [], [] ] ]
theta_p_No_t=[ [ [], [], [] ], [ [], [], [] ], [ [], [], [] ] ]
theta_p_No_tb=[ [ [], [], [] ], [ [], [], [] ], [ [], [], [] ] ]
theta_p_No_tt=[ [ [], [], [] ], [ [], [], [] ], [ [], [], [] ] ]
theta_p_Sig=[ [ [], [], [] ], [ [], [], [] ], [ [], [], [] ] ]
```

```
for i in range(len(theta_Full[0][0])):
    theta_p_Full[0][0].append(theta_Full[0][0][i]*theta_Full[1][0][i])
    theta_p_Full[0][1].append(theta_Full[0][0][i]*theta_Full[1][1][i])
    theta_p_Full[0][2].append(theta_Full[0][0][i]*theta_Full[1][2][i])

    theta_p_Full[1][0].append(theta_Full[0][1][i]*theta_Full[1][0][i])
    theta_p_Full[1][1].append(theta_Full[0][1][i]*theta_Full[1][1][i])
    theta_p_Full[1][2].append(theta_Full[0][1][i]*theta_Full[1][2][i])

    theta_p_Full[2][0].append(theta_Full[0][2][i]*theta_Full[1][0][i])
    theta_p_Full[2][1].append(theta_Full[0][2][i]*theta_Full[1][1][i])
    theta_p_Full[2][2].append(theta_Full[0][2][i]*theta_Full[1][2][i])

for i in range(len(theta_No_t[0][0])):
    theta_p_No_t[0][0].append(theta_No_t[0][0][i]*theta_No_t[1][0][i])
    theta_p_No_t[0][1].append(theta_No_t[0][0][i]*theta_No_t[1][1][i])
    theta_p_No_t[0][2].append(theta_No_t[0][0][i]*theta_No_t[1][2][i])

    theta_p_No_t[1][0].append(theta_No_t[0][1][i]*theta_No_t[1][0][i])
    theta_p_No_t[1][1].append(theta_No_t[0][1][i]*theta_No_t[1][1][i])
    theta_p_No_t[1][2].append(theta_No_t[0][1][i]*theta_No_t[1][2][i])


    theta_p_No_t[2][0].append(theta_No_t[0][2][i]*theta_No_t[1][0][i])
    theta_p_No_t[2][1].append(theta_No_t[0][2][i]*theta_No_t[1][1][i])
    theta_p_No_t[2][2].append(theta_No_t[0][2][i]*theta_No_t[1][2][i])

for i in range(len(theta_No_tb[0][0])):
    theta_p_No_tb[0][0].append(theta_No_tb[0][0][i]*theta_No_tb[1][0][i])
    theta_p_No_tb[0][1].append(theta_No_tb[0][0][i]*theta_No_tb[1][1][i])
    theta_p_No_tb[0][2].append(theta_No_tb[0][0][i]*theta_No_tb[1][2][i])

    theta_p_No_tb[1][0].append(theta_No_tb[0][1][i]*theta_No_tb[1][0][i])
    theta_p_No_tb[1][1].append(theta_No_tb[0][1][i]*theta_No_tb[1][1][i])
    theta_p_No_tb[1][2].append(theta_No_tb[0][1][i]*theta_No_tb[1][2][i])

    theta_p_No_tb[2][0].append(theta_No_tb[0][2][i]*theta_No_tb[1][0][i])
    theta_p_No_tb[2][1].append(theta_No_tb[0][2][i]*theta_No_tb[1][1][i])
    theta_p_No_tb[2][2].append(theta_No_tb[0][2][i]*theta_No_tb[1][2][i])

for i in range(len(theta_No_tt[0][0])):
    theta_p_No_tt[0][0].append(theta_No_tt[0][0][i]*theta_No_tt[1][0][i])
    theta_p_No_tt[0][1].append(theta_No_tt[0][0][i]*theta_No_tt[1][1][i])
    theta_p_No_tt[0][2].append(theta_No_tt[0][0][i]*theta_No_tt[1][2][i])

    theta_p_No_tt[1][0].append(theta_No_tt[0][1][i]*theta_No_tt[1][0][i])
    theta_p_No_tt[1][1].append(theta_No_tt[0][1][i]*theta_No_tt[1][1][i])
    theta_p_No_tt[1][2].append(theta_No_tt[0][1][i]*theta_No_tt[1][2][i])



    theta_p_No_tt[2][0].append(theta_No_tt[0][2][i]*theta_No_tt[1][0][i])
    theta_p_No_tt[2][1].append(theta_No_tt[0][2][i]*theta_No_tt[1][1][i])
    theta_p_No_tt[2][2].append(theta_No_tt[0][2][i]*theta_No_tt[1][2][i])

for i in range(len(theta_Sig[0][0])):
    theta_p_Sig[0][0].append(theta_Sig[0][0][i]*theta_Sig[1][0][i])
    theta_p_Sig[0][1].append(theta_Sig[0][0][i]*theta_Sig[1][1][i])
    theta_p_Sig[0][2].append(theta_Sig[0][0][i]*theta_Sig[1][2][i])
```

```
    theta_p_Sig[1][0].append(theta_Sig[0][1][i]*theta_Sig[1][0][i])
    theta_p_Sig[1][1].append(theta_Sig[0][1][i]*theta_Sig[1][1][i])
    theta_p_Sig[1][2].append(theta_Sig[0][1][i]*theta_Sig[1][2][i])

    theta_p_Sig[2][0].append(theta_Sig[0][2][i]*theta_Sig[1][0][i])
    theta_p_Sig[2][1].append(theta_Sig[0][2][i]*theta_Sig[1][1][i])
    theta_p_Sig[2][2].append(theta_Sig[0][2][i]*theta_Sig[1][2][i])

av_p_Full=[ [ [], [], [] ], [ [], [], [] ], [ [], [], [] ] ]
av_p_No_t= [ [ [], [], [] ], [ [], [], [] ], [ [], [], [] ] ]
av_p_No_tb=[ [ [], [], [] ], [ [], [], [] ], [ [], [], [] ] ]
av_p_No_tt=[ [ [], [], [] ], [ [], [], [] ], [ [], [], [] ] ]
av_p_Sig=[ [ [], [], [] ], [ [], [], [] ], [ [], [], [] ] ]


for i in range(len(theta_p_No_t)):
    for j in range(len(theta_p_No_t[i])):
        av_p_Full[i][j].append(np.average(theta_p_Full[i][j]))
        av_p_No_t[i][j].append(np.average(theta_p_No_t[i][j]))
        av_p_No_tb[i][j].append(np.average(theta_p_No_tb[i][j]))
        av_p_No_tt[i][j].append(np.average(theta_p_No_tt[i][j]))
        av_p_Sig[i][j].append(np.average(theta_p_Sig[i][j]))

av_p_No_t_w=np.multiply(av_p_No_t, Sigma[0])
av_p_No_tb_w=np.multiply(av_p_No_tb, Sigma[1])
av_p_No_tt_w=np.multiply(av_p_No_tt, Sigma[2])
av_p_Sig_w=np.multiply(av_p_Sig, Sigma[3])

av_p_No_int=[[0,0,0], [0,0,0], [0,0,0]]
for i in range(len(av_p_No_int)):
    for j in range(len(av_p_No_int[i])):
        av_p_No_int[i][j]=(av_p_No_t_w[i][j]+ av_p_No_tb_w[i][j]-av_p_No_tt_w[i][j]+av_p_Sig_w[i][j])/Sigma_No_int

n_C_No_int=-9/Sigma_No_int
n_C_Full=-9/Sigma_Full
C_No_int=np.multiply(n_C_No_int, av_p_No_int)
C_Full=np.multiply(n_C_Full, av_p_Full)

#uncertainties for the coefficients, standard error

#The B coefficients
std_theta_Full=[ [ [], [], [] ], [ [], [], [] ]]
std_theta_No_t=[ [ [], [], [] ], [ [], [], [] ]]
std_theta_No_t_bar=[ [ [], [], [] ], [ [], [], [] ]]
std_theta_No_tt=[ [ [], [], [] ], [ [], [], [] ]]
std_theta_Signal=[ [ [], [], [] ], [ [], [], [] ]]

for i in range(len(theta_Full)):
    for j in range(len(theta_Full[i])):
        std_theta_Full[i][j].append(np.std(theta_Full[i][j],  ddof=1))
        std_theta_No_t[i][j].append(np.std(theta_No_t[i][j],  ddof=1))
        std_theta_No_t_bar[i][j].append(np.std(theta_No_tb[i][j],  ddof=1))
        std_theta_No_tt[i][j].append(np.std(theta_No_tt[i][j],  ddof=1))
        std_theta_Signal[i][j].append(np.std(theta_Sig[i][j],  ddof=1))

std_av_theta_No_t_w=np.multiply(std_theta_No_t, Sigma[0])
std_av_theta_No_t_bar_w=np.multiply(std_theta_No_t_bar, Sigma[1])
std_av_theta_No_tt_w=np.multiply(std_theta_No_tt, Sigma[2])
std_av_theta_Signal_w=np.multiply(std_theta_Signal, Sigma[3])
```

```
std_No_int=[ [0, 0, 0], [0, 0, 0]]
for i in range(len(std_av_theta_No_t_w)):
    for j in range(len(std_av_theta_No_t_w[i])):
        std_No_int[i][j]=np.sqrt((std_av_theta_No_t_w[i][j])**2
        + (std_av_theta_No_t_bar_w[i][j])**2 + (std_av_theta_No_tt_w[i][j])**2
        +(std_av_theta_Signal_w[i][j])**2) /Sigma_No_int


B_No_int_std=np.multiply(std_No_int, n_B_No_int)
B_full_std=np.multiply(std_theta_Full, n_B_Full)
u=1/np.sqrt(1000000)
std_err_B_No_int=np.multiply(B_No_int_std, u )
std_err_B_Full=np.multiply(B_full_std, u)

#The C coefficients
std_products_Full=[ [ [], [], [] ], [ [], [], [] ], [ [], [], [] ] ]
std_products_No_t=[ [ [], [], [] ], [ [], [], [] ], [ [], [], [] ] ]
std_products_No_t_bar=[ [ [], [], [] ], [ [], [], [] ], [ [], [], [] ] ]
std_products_No_tt=[ [ [], [], [] ], [ [], [], [] ], [ [], [], [] ] ]
std_products_Signal=[ [ [], [], [] ], [ [], [], [] ], [ [], [], [] ] ]

for i in range(len(theta_p_No_t)):
    for j in range(len(theta_p_No_t[i])):
        std_products_Full[i][j].append(np.std(theta_p_Full[i][j]))
        std_products_No_t[i][j].append(np.std(theta_p_No_t[i][j]))
        std_products_No_t_bar[i][j].append(np.std(theta_p_No_tb[i][j]))
        std_products_No_tt[i][j].append(np.std(theta_p_No_tt[i][j]))
        std_products_Signal[i][j].append(np.std(theta_p_Sig[i][j]))

std_products_No_t_w=np.multiply(std_products_No_t, Sigma[0])
std_products_No_t_bar_w=np.multiply(std_products_No_t_bar, Sigma[1])
std_products_No_tt_w=np.multiply(std_products_No_tt, Sigma[2])
std_products_Signal_w=np.multiply(std_products_Signal, Sigma[3])

std_No_int_C=[ [0, 0, 0], [0, 0, 0], [0, 0, 0]]
for i in range(len(std_products_No_t_w)):
    for j in range(len(std_products_No_t_w[i])):
        std_No_int_C[i][j]=np.sqrt((std_products_No_t_w[i][j])**2
        +(std_products_No_t_bar_w[i][j])**2 + (std_products_No_tt_w[i][j])**2
        +(std_products_Signal_w[i][j])**2)/Sigma_No_int

C_No_int_std=np.multiply(std_No_int_C, n_C_No_int)
C_Full_std=np.multiply(std_products_Full, n_C_Full)
std_err_C_No_int=np.multiply(C_No_int_std,u)
std_err_C_Full=np.multiply(C_Full_std, u)
```

A.5 Histograms for the leptonic angular distributions

```
#Function for plotting the distributions.
#(0,0)=k+, (0,1)=n+, (0,2)=r+, (1,0)=k-, (1,1)=n-, (1,2)=r-

def Hist(i,j):
    F=theta_Full[i][j]
    t=theta_No_t[i][j]
    t_b=theta_No_tb[i][j]
    tt=theta_No_tt[i][j]
    S=theta_Sig[i][j]
```

```
W_F=np.ones_like(F)*Sigma_Full
W_t=np.ones_like(t)*Sigma[0]
W_t_b=np.ones_like(t_b)*Sigma[1]
W_tt=np.ones_like(tt)*Sigma[2]
W_S=np.ones_like(S)*Sigma[3]


Bins_0=np.arange(-1,1.01,0.01) # Gives 200 Bins spaced between -1 and +1

H_F, Bins_F=np.histogram(F, bins=Bins_0, weights=W_F, density=True) #The Full is normalized


#The processes are weighted and binned
H_t, Bins_t=np.histogram(t, bins=Bins_0, weights=W_t)
H_t_b, Bins_t_b=np.histogram(t_b, bins=Bins_0, weights=W_t_b)
H_tt, Bins_tt=np.histogram(tt, bins=Bins_0, weights=W_tt)
H_s, Bins_s=np.histogram(S, bins=Bins_0, weights=W_S)

#Adding and subtracting the frequencies in the bins accordingly
H_N=(H_t+H_t_b-H_tt+H_s)

#Defining the left edges and the width for the bar graph
left_edges = Bins_s[:-1]
Width = (left_edges[1] - left_edges[0])


#Normalizing the combinations
Norm_factor=1/np.sum(H_N*np.diff(Bins_s))
H_NN=H_N*Norm_factor #Normalizing the combination

#Error bars
Err_F=np.std(H_F, ddof=1)/np.sqrt(len(H_F))
Err_N=np.std(H_NN, ddof=1)/np.sqrt(len(H_NN))

def getRatio(bin1,bin2):
    bins = []
    for b1,b2 in zip(bin1,bin2):
        if b1==0 and b2==0:
            bins.append(1.)
        elif b2==0:
            bins.append(0.)
        else:
            bins.append(float(b1)/float(b2))
    return bins

fig = plt.figure()
ax = fig.add_subplot(2,1,1)
plt.xticks(fontsize=20)
plt.yticks(fontsize=20)

#Plotting the histograms

ax.bar(left_edges, H_NN, align='edge', width=Width, color='r',
       alpha=0.5,yerr=Err_N, ecolor='r', label='No Interference', capsize=1)
ax.bar(left_edges, H_F, align='edge', width=Width, color='b',
       alpha=0.5, yerr=Err_F, ecolor='b', label='Full',capsize=1)
leg = ax.legend( loc="best", fontsize=14)
ax.set_ylabel(r'$\frac{1}{\sigma}\frac{d\sigma}{dcos(\theta_{+}^{k})}$', fontsize=28)
ax.set_title(r'Distribution of $cos(\theta_{+}^{k})$ ', fontsize=28)
```

```
# Setting up the subplot for ratio

ax = fig.add_subplot(2,1,2)
plt.xticks(fontsize=20)
plt.yticks(fontsize=20)
ratio = getRatio(H_NN,H_F)
#1 for reference
one=np.ones_like(ratio)

#the upper and lower uncertainties
bin_err_r_u=ratio*((Err_N/H_NN)+(Err_F/H_F))
ratio_err_upper=ratio+bin_err_r_u
ratio_err_lower=ratio-bin_err_r_u

#plotting the ratio

ax.plot(left_edges,ratio, color='m', label='No Interference/Full')
ax.plot(left_edges, one, color='k', label='1')
ax.plot(left_edges, ratio_err_upper, color='b', label='Upper uncertainty ')
ax.plot(left_edges, ratio_err_lower, color='r', label='Lower uncertainty ')
leg=ax.legend(loc="best", fontsize=14)
ax.set_ylim(0.5,1.5)
ax.set_xlabel(r'$cos(\theta_{+}^{k})$',fontsize=25)
ax.set_ylabel('Ratio', fontsize=28)
```

References

[1] *Measurement of the top-quark mass in t t-bar events with lepton+jets final states in pp collisions at sqrt(s)=8 TeV*. Tech. rep. Geneva: CERN, 2014. arXiv: 1905.02302 [hep-ex].

[2] et al. M. Sirunyan. "Measurement of the top quark Yukawa coupling from $t\bar{t}$ kinematic distributions in the dilepton final state in proton-proton collisions at $\sqrt{s} = 13$ TeV". In: *Physical Review D* 102.9 (Nov. 2020). arXiv: 2009.07123v3 [hep-ex].

[3] M. Carena and C. E. M. Wagner. "The Infrared Fixed Point of the Top Quark Mass and its Implications within the MSSM". In: (1994). arXiv: hep-ph/9407208.

[4] et al. T. Aaltonen. "Direct Measurement of the Total Decay Width of the Top Quark". In: *Physical Review Letters* 111.20 (Nov. 2013). arXiv: 1308.4050v2 [hep-ex].

[5] et al. S.Abachi. "Observation of the Top Quark". In: *Phys. Rev. Lett.* 74 (14 Apr. 1995), pp. 2632–2637. arXiv: hep-ex/9503003.

[6] W. Bernreuther et al. "Top-Quark Spin Correlations at Hadron Colliders: Predictions at Next-to-Leading Order QCD". In: *Physical Review Letters* 87.24 (Nov. 2001). ISSN: 1079-7114. arXiv: hep-ph/0107086.

[7] W. Bernreuther et al. "Spin properties of top quark pairs produced at hadron colliders". In: *Acta Phys. Polon. B* 34 (2003). Ed. by K. Fialkowski, M. Jezabek, and M. Rozanska, pp. 4477–4490. arXiv: hep-ph/0304244.

[8] W. Bernreuther et al. "Next-to-leading order QCD corrections to top quark spin correlations at hadron colliders: the reactions $gg \longrightarrow t\bar{t}$ and $gg(\bar{q}) \longrightarrow t\bar{t}q(\bar{q})$." In: *Physics Letters B* 509.1-2 (June 2001), pp. 53–58. ISSN: 0370-2693. arXiv: hep-ph/0104096.

[9] Werner Bernreuther and Zong-Guo Si. "Top quark spin correlations and polarization at the LHC: Standard model predictions and effects of anomalous top chromo moments". In: *Physics Letters B* 725.1-3 (Aug. 2013), pp. 115–122. ISSN: 0370-2693. arXiv: 1305.2066 [hep-ex].

[10] Werner Bernreuther, Dennis Heisler, and Zong-Guo Si. "A set of top quark spin correlation and polarization observables for the LHC: Standard Model predictions and new physics contributions". In: *Journal of High Energy Physics* 2015.12 (Dec. 2015), pp. 1–36. ISSN: 1029-8479. arXiv: 1508.05271 [hep-ex].

[11] Rikkert Frederix, Ioannis Tsinikos, and Timea Vitos. "Probing the spin correlations of $t\bar{t}$ production at NLO QCD+EW". In: *The European Physical Journal C* 81.9 (Sept. 2021). arXiv: 2105.11478v2 [hep-ex].

[12] Morad Aaboud et al. "Measurements of top quark spin observables in $t\bar{t}$ events using dilepton final states in $\sqrt{s} = 8$ TeV pp collisions with the ATLAS detector". In: *JHEP* 03 (2017), p. 113. arXiv: 1612.07004 [hep-ex].

[13] Albert M Sirunyan et al. "Measurement of the top quark polarization and $t\bar{t}$ spin correlations using dilepton final states in proton-proton collisions at $\sqrt{s} = 13$ TeV". In: *Phys. Rev. D* 100.7 (2019), p. 072002. arXiv: 1907.03729 [hep-ex].

[14] Werner Bernreuther and Arnd Brandenburg. "Tracing CP violation in the production of top quark pairs by multiple TeV proton-proton collisions". In: *Physical Review D* 49.9 (May 1994), pp. 4481–4492. arXiv: hep-ph/9312210v1.

[15] J. Alwall et al. "The automated computation of tree-level and next-to-leading order differential cross sections, and their matching to parton shower simulations". In: *Journal of High Energy Physics* 2014.7 (July 2014). ISSN: 1029-8479. arXiv: 1405.0301v2 [hep-ex].

[16] Johan Alwall et al. "A Standard format for Les Houches event files". In: *Comput. Phys. Commun.* 176 (2007), pp. 300–304. arXiv: hep-ph/0609017.

[17] J. Butterworth et al. "Les Houches 2013: Physics at TeV Colliders: Standard Model Working Group Report". In: (May 2014). arXiv: 1405.1067 [hep-ex].